Downhole Seismic Imaging for mineral exploration

VSP survey at Cadieux, Renfrew, Ontario

Compiled by

Erick Adam and Gervais Perron

with contributions from

Kristen Beaty, Kristine Butler, Greg Clarke, Karen Pflug, Dave Eaton, Dave Forsyth, Ian Kay, Jonathan Mwenifumbo, Matthew Salisbury, and Brian Roberts

Geological Survey of Canada
Continental Geoscience Division
Seismology and Electromagnetism Section
1 Observatory Crescent
Ottawa, Ontario
K1A 0Y3

January 16^{th} 1998
Updated April 27^{th} 1998

Contents

1 Summary

A vertical seismic profiling survey was conducted in hole CA-96-01G on the Cadieux Property near Renfrew (Ontario) from October 29 to October 31, 1997. The objective was to test a new downhole receiver module and to verify the seismic reflectivity of a known mineralized zone on the property. Data interpretation, based on *in situ* and laboratory physical rock property measurements have confirmed that disseminated sulphides generate a strong reflection. A pegmatite unit also appears to be very reflective. This study demonstrates that seismic reflection can be used to map the mineralized zone at depths exceeding 500 m.

2 Introduction and motivation

A vertical seismic profiling (VSP) survey was conducted at Cadieux to test the downhole receiver prototype developed by Geophysical Survey Systems of Houston. The test site location was chosen because of its proximity to Ottawa, the availability of deep boreholes, and the presence of sulphide mineralization. In parallel, a comprehensive rock property study was undertaken. Both *in situ* and laboratory physical rock properties were measured in a borehole and on representative core samples. The acoustic impedances of the rock units encountered at Cadieux, derived from the rock property study, allow us to link reflections observed on the VSP section with rock units and structures intersected by the borehole.

This report summarizes the VSP data acquisition, data processing, and the physical rock property study. An interpretation of the data, based on available geological and geophysical data is also presented.

3 Location and access

The Cadieux Property is located about 100 km west of Ottawa and 7 km south of the town of Renfrew (Figure 1) in Admaston Township, Renfrew County, Ontario.

Access to the property is by paved road (Pucker Street) and dirt road (Admaston road and other private gravel roads).

4 Geological setting

The Cadieux property consists of a metasedimentary and metavolcanic sequence comprised of marble, paragneiss,and volcanic rocks of Grenvillian age. Mineralization is hosted by a sequence of siliceous and dolomitic marbles overlying a volcanic complex. Five main zones of sphalerite have been outlined on the property, the Swamp Zone being the largest with an estimated 496 tonnes grading 8.3% Zn and 0.33% Pb. Its thickness varies between

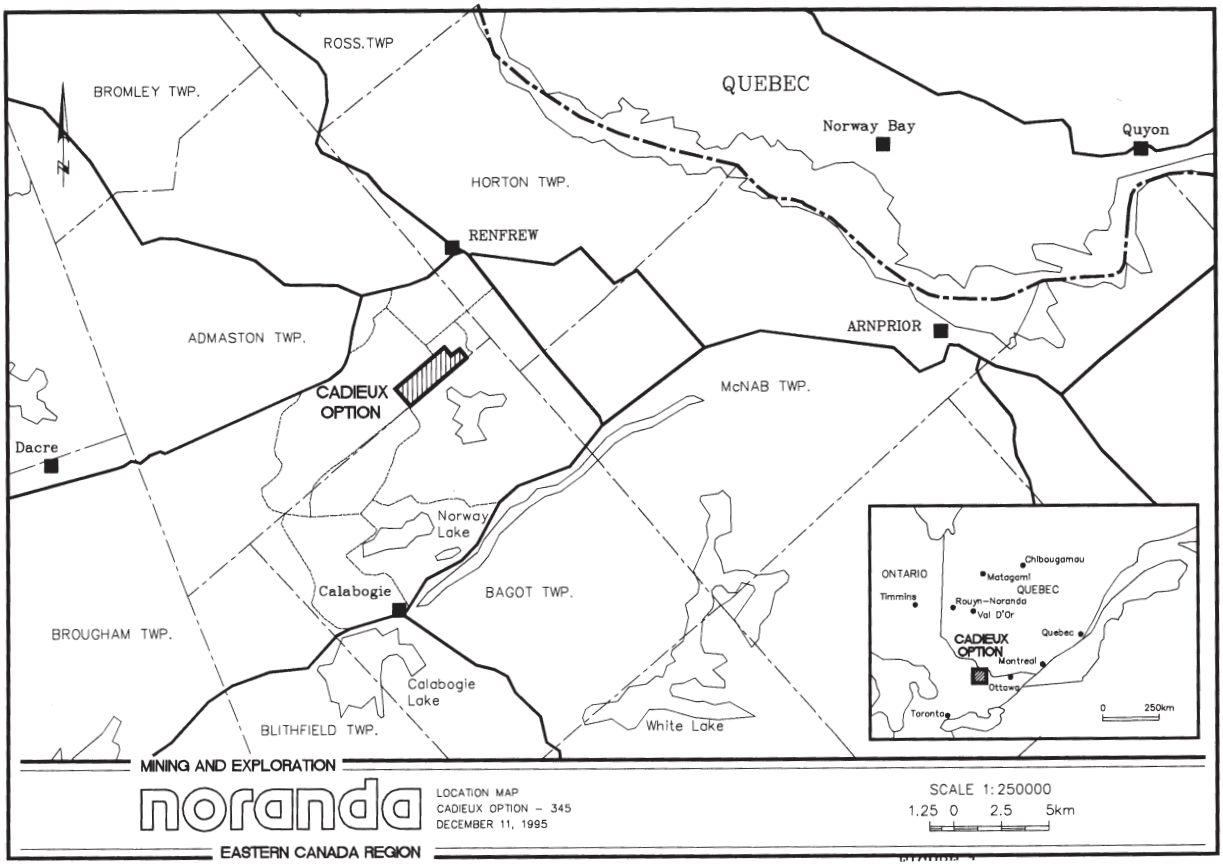

Figure 1: Location map.

2.3 and 26.4 m and it dips at 45^o to the northeast to depths exceeding 800 m. Most of the mineralization is concentrated in the hinge area of controlling folds giving the orebody a cylindrical shape (Roger 1996).

5 Data Acquisition

Data were acquired using a single, 3-component receiver unit consisting of orthogonal 30 Hz natural frequency geophones. The receiver unit was clamped to the borehole using a metallic band. The seismic signal was digitized in the recording truck using a state-of-the-art 24 bit seismograph (OYO DAS-1).

In this report, the axial component (parallel to the borohole axis) is referred to as the vertical or Z component. Obviously, this component will be truly vertical only if the borehole is vertical. The two other components are referred to as horizontal (H1 and H2) and they will

be truly horizontal only where the borehole is vertical.

5.1 Overview

October 29^{th} 1997

The Downhole Seismic Imaging (DSI) data acquisition took place from October 29^{th} through October 31^{st} 1997. The original plan was to record DSI data in the most recent exploration borehole on the Cadieux property (CA-97-01). This BQ size (60 mm diameter) hole is 1200 m deep and intersects the "Swamp Zone" at a depth of 850 m. Just 2 days before the survey a storm struck the region, leaving 25 cm of snow on the ground making access to the borehole difficult (Figure 2). Furthermore, dummy-probing the hole revealed an obstruction at a depth of 220 m. This was unexpected as drilling had been completed only 2 days before.

We decided to use borehole CA-96-01G which was located about 1 km away from borehole CA-97-01. This second hole was easily accessible and multiparameter logging had been completed a few days before, but it was only 560 m deep and intersected only the top of the Swamp Zone. Thus, the sulphide zone intersected by this borehole is low-grade compared with other sulphide zones. Since, no shooting pit was available at this site, all the shots recorded on the first day were fired in a dry swamp consisting mainly of a thick layer of peat. On the first day of shooting many acquisition parameters were tested such as clamping strength, charge size, triggering systems and sampling rate. From the beginning we were confronted by strong electrical noise (60 Hz and numerous harmonics) obscuring most of the signal and with bad source coupling.

October 30^{th} 1997

On the second day of acquisition a shooting pit was dug approximately 75 m away from the borehole. The natural water filling rate was slow and after only a few shots the hole dried up and source coupling once again became inadequate. On that day, 36 shots were recorded at depths ranging from 100 m to 208 m. We also observed that the electrical noise level (60 Hz and several harmonics) was increasing as a function of the probe depth and, at 208 m, the first break energy was completely masked by electrical noise. The source of electrical noise is discussed later.

October 31^{st} 1997

At the beginning of the third day, the shooting hole was filled with more than 48 cubic meters of water. The remainder of the borehole was logged using a spacing of 4 m and 90 g charges fired every 2 or 3 minutes. The source coupling was greatly improved by the water

in the shooting pit. The acquisition parameters are summarized in Table 1.

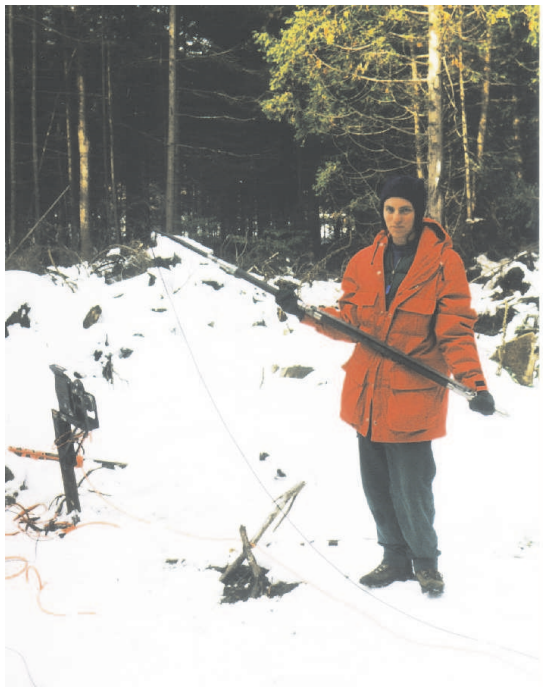

Figure 2: Pictures taken during data acquisistion: the recording truck, a dynamite shot and the downhole receiver unit.

	October 29^{th}	October 30^{th}	October 31^{st}
Number of shots	6	36	88
Depth coverage	75-175 m	100-208 m	212-532 m
Receiver spacing	25 m	4 m	4 m
Shot charge	90-180-270-360 g	90 g	90 g
Pit conditions	Dry pit (swamp)	Dry pit (glacial till)	Water filled pit
Source coupling	Poor	Poor	Good to acceptable
Sampling rate	1 ms	0.5 ms	0.5 ms
Recording time	2 s	2 s	2 s
Noise level	Acceptable	High	High

Table 1: Acquisition parameters

5.2 Tests

Last minute changes to our initial plan forced us to use different kinds of shooting pits. Results from these tests show that only the water-filled pit achieved good coupling. The water helps to send more energy into the ground.

Another test was done to define the optimum charge size. In good coupling conditions, 90 g charges proved to be adequate up to the maximum depth of 532 m. More powerful charges (up to 270 g) can be used to compensate for the deterioration of the shooting pit (caused by the collapsing sidewalls).

5.3 Electrical noise

As mentioned previously, every record suffered from electrical noise contamination (60 Hz and harmonics). The nature of the noise is puzzling since the amplitude and the phase are not constant on every channel (component). There is also a variation of the amplitude associated with the receiver-to-mineralization distance. The amplitude of the noise increased as the probe got closer to the Swamp Zone. It is thus possible that the source of the noise could be associated with the presence of mineralization. A current induced in a conductor such as an ore body would produce fluctuations in the surrounding magnetic field affecting the geophones in the probe. The difference in amplitude and phase between channels could be explained by the different geophone orientations with respect to the magnetic field variations.

6 Data Processing

Processing of the Cadieux VSP data was performed on a Unix workstation using the ITA/Insight processing package. A standard VSP processing sequence has been used to process the Cadieux data and a complete description of VSP processing techniques is presented

by Hardage (1985). In this section, only the processing aspects specific to the Cadieux data are discussed in detail.

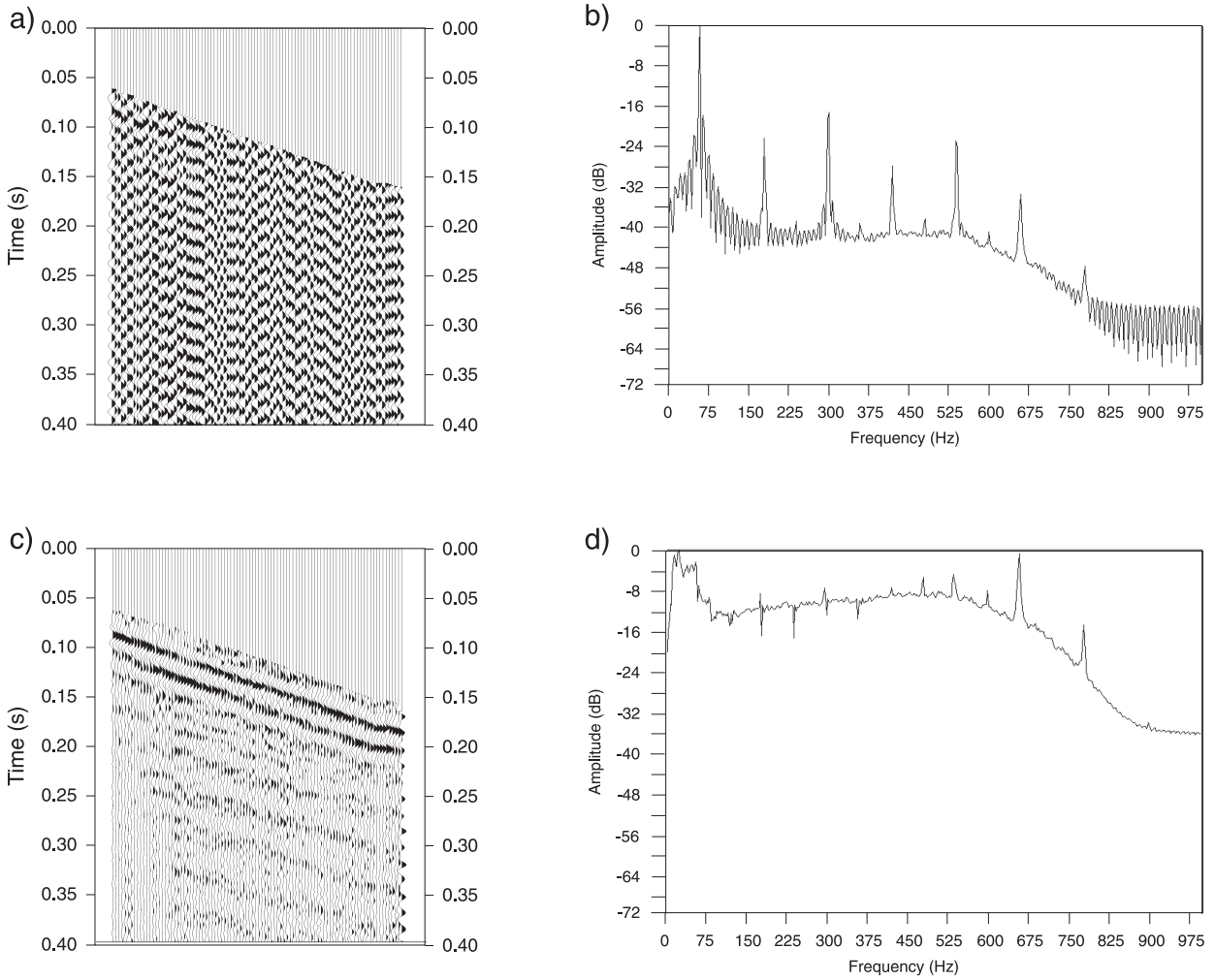

Figure 3: Vertical component of the raw data (a) and its amplitude spectrum (b) revealing the presence of strong 60 Hz and its harmonics. c) Same as (a) but after removal of electrical noise with an adaptive filtering method; the amplitude spectrum of the filtered data (d) shows that the electrical noise is considerably reduced.

6.1 Noise removal

The only cultural noise was of electrical nature and was not generated by the acquisition equipment. Besides the electrical noise, the area was quiet and ongoing diamond drilling about 1 km away from the survey site did not appear to affect seismic data quality.

Figure 3a shows the raw data recorded by the vertical component to which a 20/30-120/160 Hz bandpass filter has been applied for display. The amplitude spectrum (Figure 3b) reveals that the traces are dominated by strong electrical noise making identification of the first break time impossible. It also made data quality control difficult during the acquisition. These data were contaminated mainly by 60 Hz but other harmonics (180, 300, 420, 540, 660 Hz etc.) were also present. This noise is usually removed by applying several notch filters in the frequency domain with the inconvenience of filter noise being added to the data at the beginning and end of each trace. Because of the low signal-to-noise ratio of the data, an alternate method was used to subtract the electrical noise. To remove noise frequencies, the exact phase and amplitude of the noise frequency is estimated by performing Discrete Fourier Transforms (DFT) at small frequency increments around the frequency to remove (Nyman and Gaiser 1983, Butler and Russell 1993, Adam and Langlois 1995). The frequency/phase pair which maximises the DFT amplitude is then subtracted from the raw data in the time domain. The data filtered using this method are shown in Figure 3c, compressional wave first breaks are now clearly visible. The amplitude spectrum (Figure 3d) shows that the electrical noise has been effectively removed. Data for the three components on which monofrequency electrical noise has been removed (60, 180, 300, 420, 540, and 660 Hz) are displayed in Figure 4.

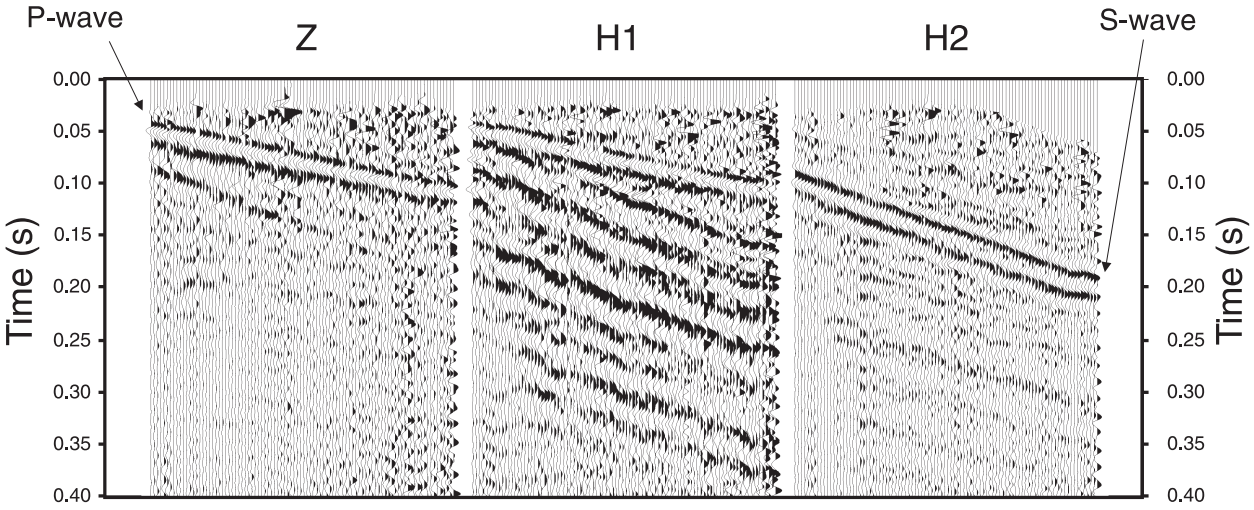

Figure 4: Filtered data from the vertical component (a) and the two horizontal components (b and c). Monofrequency electrical noise has been removed and a bandpass filter (20/30-120/150 Hz) has been applied for display. Note that no component rotations have been applied.

Monofrequency electrical noise removal	Adaptive filter (60, 180, 300, 360, 420, 540, and 660 Hz)
Frequency content analysis	Band-limited frequency panels
Geometry	
Spectral equalization	40 - 140 Hz
Sort	shot-receiver distance
Trace editing	
Remove downgoing P-wave	median velocity filter (9 points)
Remove other downgoing waves	*f-k* velocity filter
Energy balancing	0 - 500 ms window
Trace mixing	3 points (12%-75%-13%)

Table 2: P-wave processing sequence

6.2 P-wave data

Most of the P-wave energy were recorded on the Z component (Figure 4a), with some on the first horizontal component (H1). As the strongest P-wave first breaks are on the Z component, data from this geophone was processed without component rotation. There is a minor S-wave first break on the vertical component but we did not attempt to remove it. Rotating the Z component with H1 to maximise the P-wave energy on one component would also reduce the S-wave. Establishing the frequency bandwidth of the data is an important step. The band-limited frequency filter panels of the vertical component (Z) are shown in Figure 5 and demonstrates that frequencies up to 200 Hz were measured at all depths. Higher frequencies have lower amplitudes but reflections (up-going) are clearly visible (arrows on Figure 5). The processing sequence was applied to the P-wave component to enhance the up-going energy by attenuating the downgoing waves: P-wave first break removal by median filtering, other downgoing wave removal by frequency-wavenumber (*f-k*) filter and trace mixing for display. The P-wave data processing sequence is summarized in Table 2.

The final processed P-wave VSP section shows 3 distinct reflections (Figure 6). Reflection labelled B projects at a depth of 518 m, and it corresponds to a 25 m thick zone of disseminated sulphides (up to 10% sphalerite and 5% pyrite). Reflection labelled A projects to a pegmatite zone which was intersected by borehole CA-96-01G between depths of 434 and 452 m. This unit is described as a hard quartz-feldspath-diopside rock with fluorite, biotite and traces of pyrite (Roger 1996). C does not project in the borehole as this reflection would intercept the borehole at a depth of 650 m and the deepest recording was done at 532 m. Thus, we can only speculate about the origin of this reflection: an amphibolite unit intercepted at 661 m is a possible candidate but another interpretation is that it could represent the bottom of the mineralized zone. A highly reflective zone has been identified in the vicinity of the borehole at about 300 m depth. This zone of high amplitudes is aligned

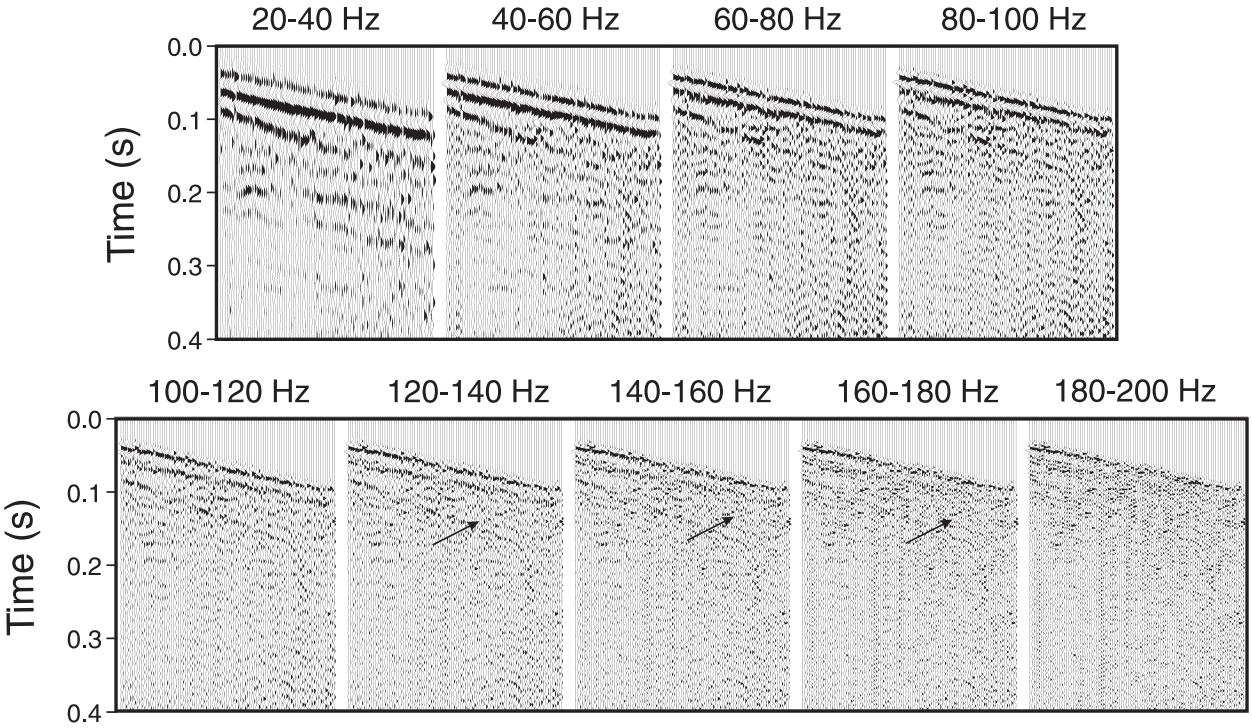

Figure 5: Summary of the frequency filter panel applied to the vertical component (Z). These panels shows that frequencies up to 200 Hz were measured at all depths. Frequency bands between 120 and 180 Hz show 2 reflections (up-going waves) indicated by the arrows.

with the pegmatite unit and it could be caused by local thickening of that unit.

6.3 S-wave data

Most of the S-wave data were on the H2 horizontal component (Figure 4c) and thus no rotation was required before processing. The band-limited filter panels (figure 7) revealed that frequencies as high as 180 Hz have been recorded. The S-wave first breaks are wider than the P-wave first breaks in all frequency bands. Also note that no obvious reflections are observed on the raw data. The processing sequence applied to the S-wave component was similar to the one used for processing the P-wave data. The S-wave data processing sequence is summarized in Table 3.

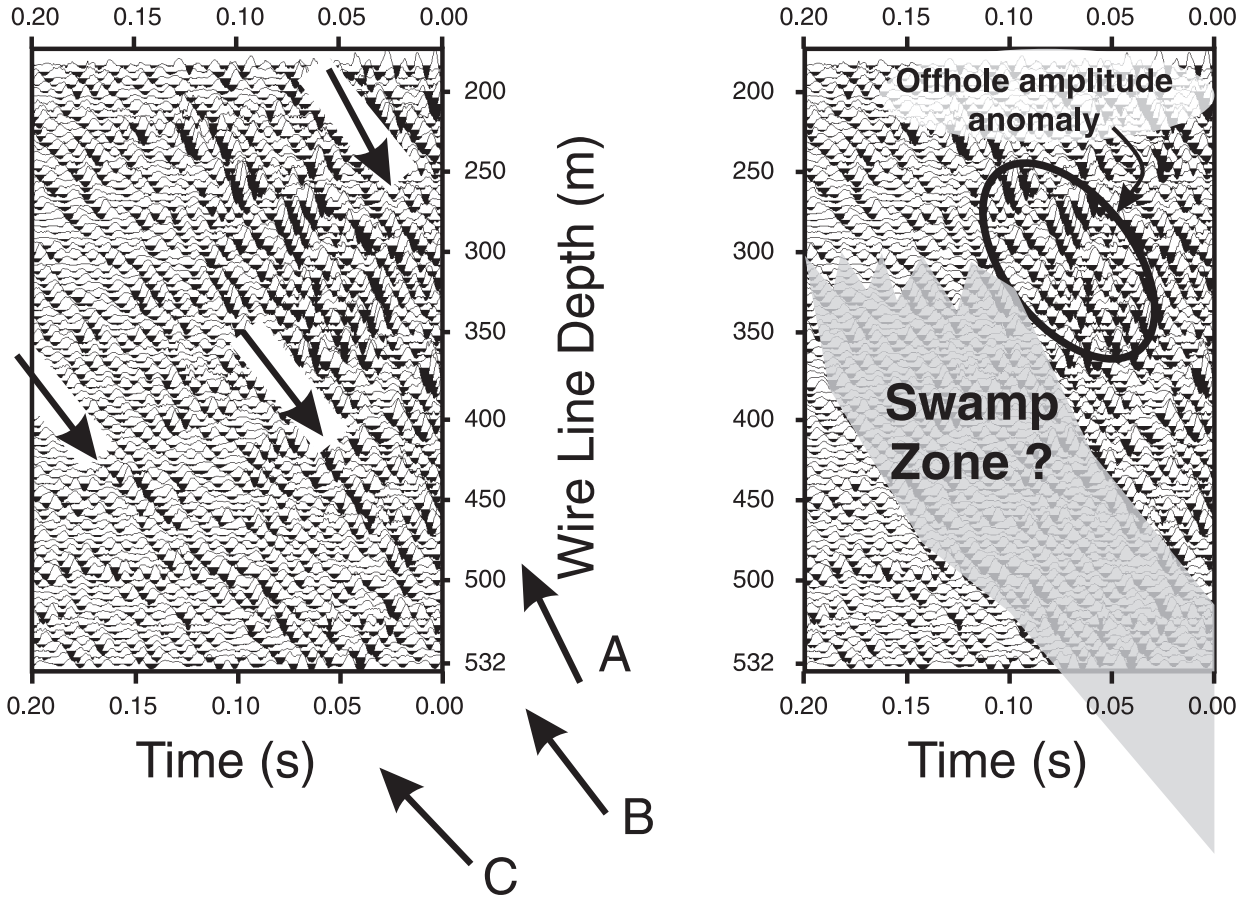

Figure 6: Final processed P-wave VSP section showing 3 distinct reflections. Reflection labelled B originates from the mineralized unit intersected by the borehole. A corresponds to a pegmatite zone while C may be caused by the base of the suphide mineralization or the amphibolite unit intercepted at 661 m.

7 Modelling

Synthetic seismic modelling of the Swamp Zone was used to design the survey and then to help interpret the VSP data. A simplified model of the orebody was built using Matlab and used for input into the Born modelling software. Modelling has shown that, because of the ore geometry (a dipping cylinder), the seismic response was not dependant on the shot location. But, data processing is often facilitated when P- and S-waves are well separated in time. Thus it is preferable to place the shot away from the borehole collar (> 100 m). In this section, the Born Approximation is outlined, the model definition is presented and finally some modelling results are shown.

Monofrequency electrical noise removal	Adaptive filter (60, 180, 300, 360, 420, 540, and 660 Hz)
Frequency content analysis	Band-limited frequency panels
Geometry	
Spectral equalization	40 - 140 Hz
Sort	shot-receiver distance
Trace editing	
Remove downgoing S-wave	median velocity filter (9 points)
Remove other downgoing waves	*f-k* velocity filter
Energy balancing	0 - 500 ms window
Trace mixing	3 points (12%-75%-13%)

Table 3: S-wave processing sequence

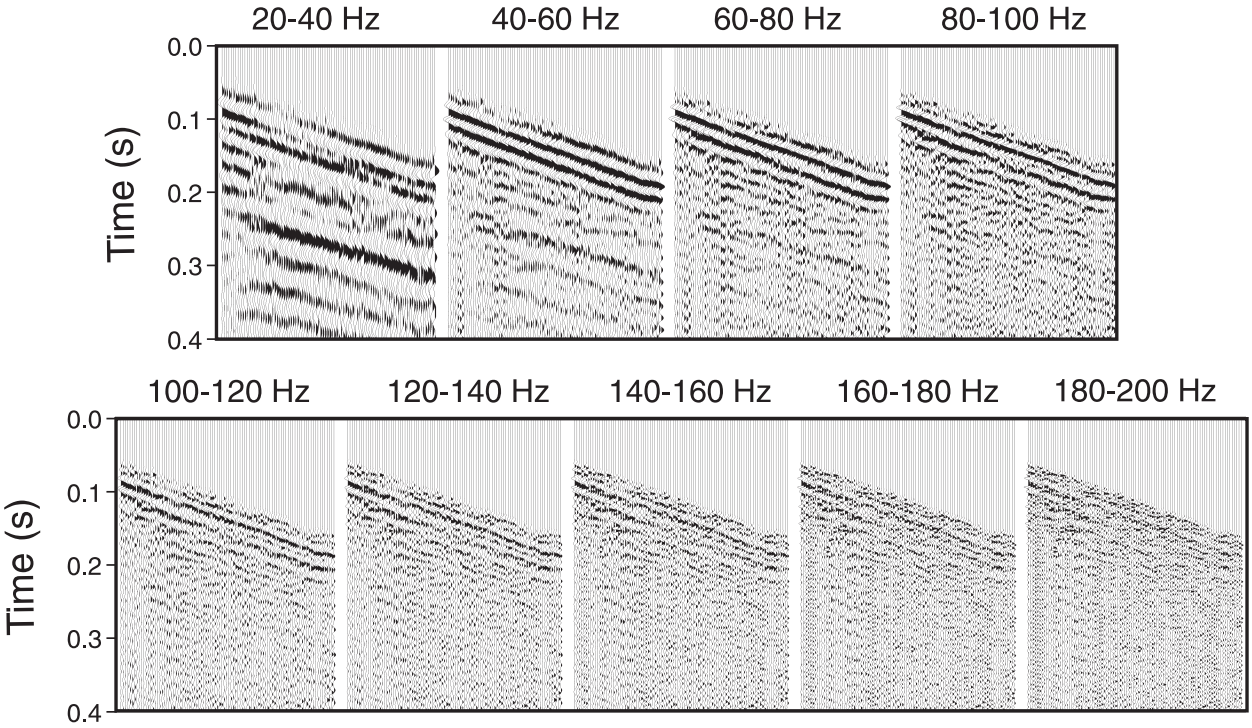

Figure 7: Summary of the frequency filter panel applied to the horizontal component (H2). These panels shows that frequencies up to 140 Hz were measured at all depths. At shallow dpths (< 250 m) frequencies as high as 180 Hz have been recorded. The frequency content of the S-wave is lower than the P-wave.

7.1 Born Approximation

The forward modelling method used in this study to obtain realistic synthetic seismic responses for particular geological models is known as the 3-D Born Approximation. This

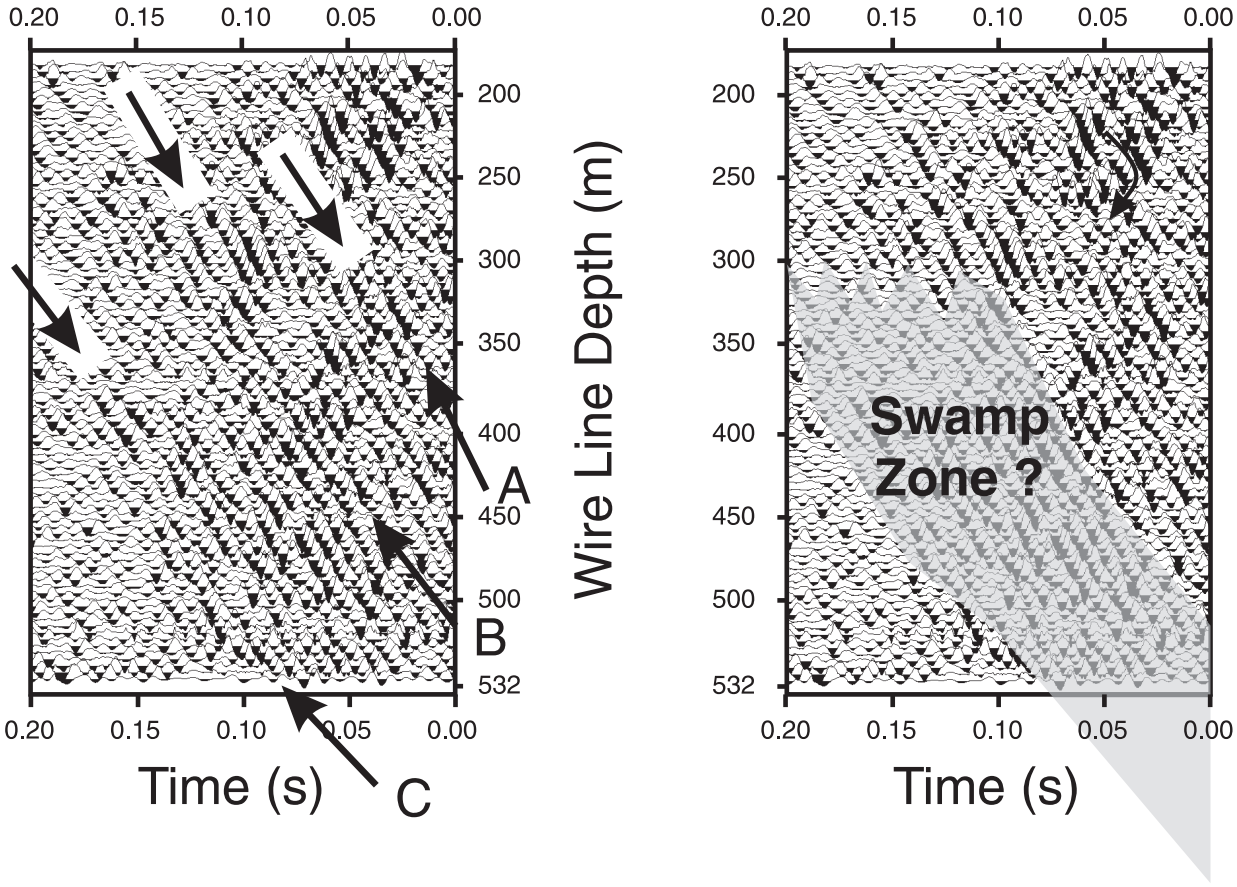

Figure 8: Final processed S-wave VSP section showing 3 distinct reflections. Reflection labelled B originates from the mineralized unit intersected by the borehole. A correspond to a pegmatite zone while C may be caused by the base of the suphide mineralization or the amphibolite unit intercepted at 661 m.

method, which is relatively straightforward, is formally based on Perturbation Theory and was originally developed to handle problems in Quantum Physics. In the seismic literature, it is most commonly invoked for dealing with random media, or for linearized inversion rather than forward modelling per se.

The Born Approximation is designed to handle geologic situations where short-wavelength anomalies are superimposed onto a smoothly varying background medium. It can be shown that, to a first approximation, the net response of the combined medium (smooth background plus anomalies) is equivalent to the response of the smooth background model taken alone, plus the sum of the scattering response from each anomalous point. The accuracy of this approximation improves if the magnitudes of the perturbations (*i.e.* relative deviation from the background medium) are small. In the models studied so far, the background

medium is assumed to be constant; it is possible, however, to relax this restriction in order to accommodate a more realistic background.

This approach differs from conventional seismic modelling methods, such as ray tracing, in a number of important respects. For example, ray tracing is most effective if the earth can be subdivided into discrete layers that are separated by smooth interfaces. Ray theory breaks down if the interfaces become highly irregular, as might be the case for ore bodies and other geological features in a mining environment. The Born Approximation places no such restrictions on the geological model. Other techniques, such as a direct solution of the wave equation by finite-differences, are currently impractical for 3-D seismic modelling.

7.2 Numerical model definition

In order to visualize the geometry of the shot and receiver locations relative to each other and to the location of the ore body, a three dimensional plot was created using MATLAB (Figure 9). Information was provided by Noranda of the azimuth and dip of the borehole at various wireline depths which were then converted to mine grid co-ordinates and true depth. Receiver locations, recorded as wire line depth, were converted to the same co-ordinates for modelling purposes by interpolating from the borehole trace. Two flat, dipping planes were used to represent the top and bottom of the predicted extent of the ore body with dips of 36 and 42 degrees respectively. A strike of zero was used for both. These values were estimated from geological cross-sections provided by Noranda, as was the area covered by the planes.

7.3 Synthetic data examples

Shown in Figure 10 are the modelling results at Cadieux using the simplified geometry of the Swamp Zone and the actual survey geometry. A background P-wave velocity of 6.1 km/s and S-wave velocity of 3.0 km /s were used. 2.8 g/cc was the background density and the Swamp zone was modelled using a 10 % density variation at its boundary.

8 Physical rock properties

Seismic waves are reflected where there are sharp acoustic impedances variations (the product of density and the seismic velocity). To identify and characterize potential reflective geological contacts, a study of the physical rock property study of the rock units encountered on the Cadieux property was undertaken. The density and P-wave velocity measurements of representative rock samples were conducted at the Dalhousie High-Pressure Laboratory. Densities and P-wave velocities were also measured *in situ* (density and full waveform sonic) by the Borehole Logging Section of the Mineral Resources Division in borehole CA-96-01G to a depth of 558 m. These measurements performed on relatively small rock samples can then be compared against the velocities estimated from the VSP P- and S-wave first breaks

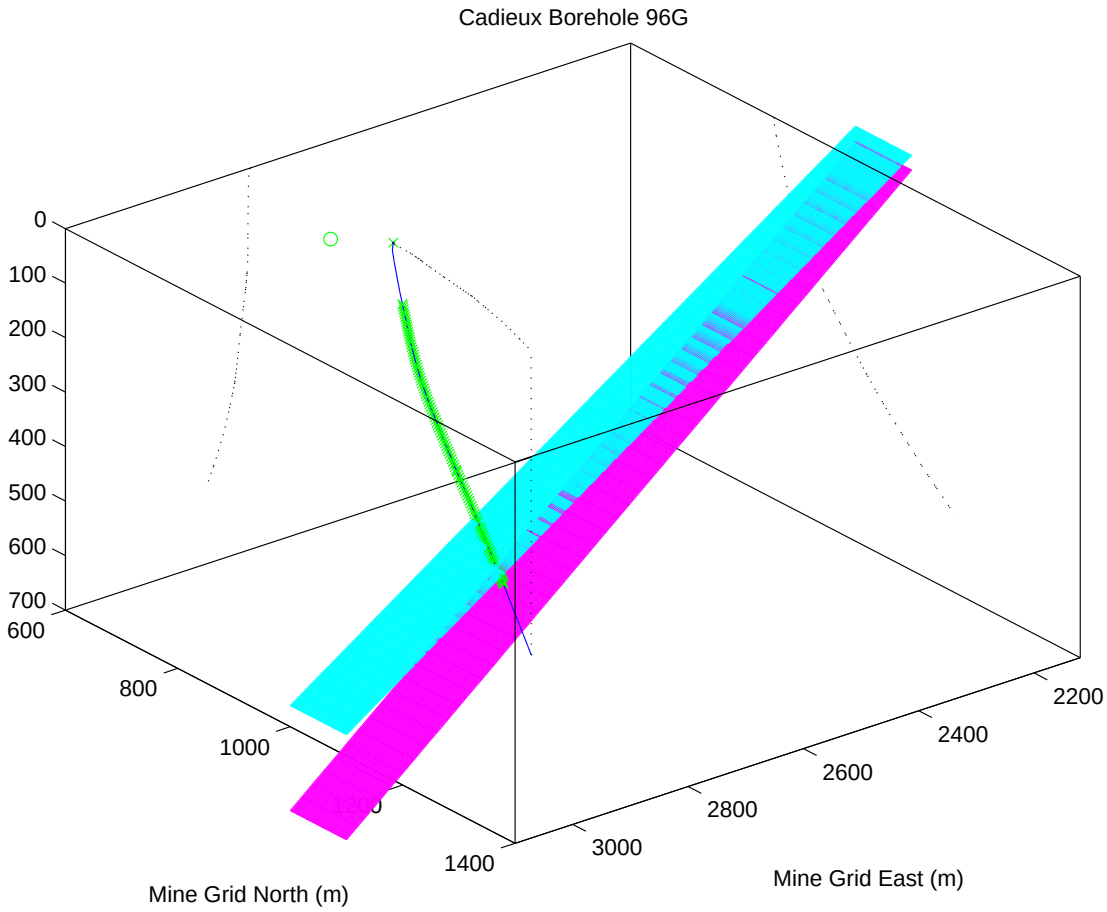

Figure 9: Plot of the survey geometry in relation to the Swamp Zone. The shot and receiver locations are indicated and the two dipping planes represent the top and the bottom of the Swamp Zone.

(Figure 11. A linear regression of the first break pick time indicates that the P-wave velocity is 6450 m/s while the S-wave velocity is 3310 m/s. Since the intercept times are quite different (18 ms for the P-wave *versus* 32 ms for the S-wave), this suggests that the S-wave is generated at the source.

8.1 Laboratory measurements

A total of 8 samples have been measured at the Dalhousie High-Pressure Laboratory. High velocities have been measured for all rock units (dolomitic marbles, marbles, and amphibolites) and are summarized in Figure 12.

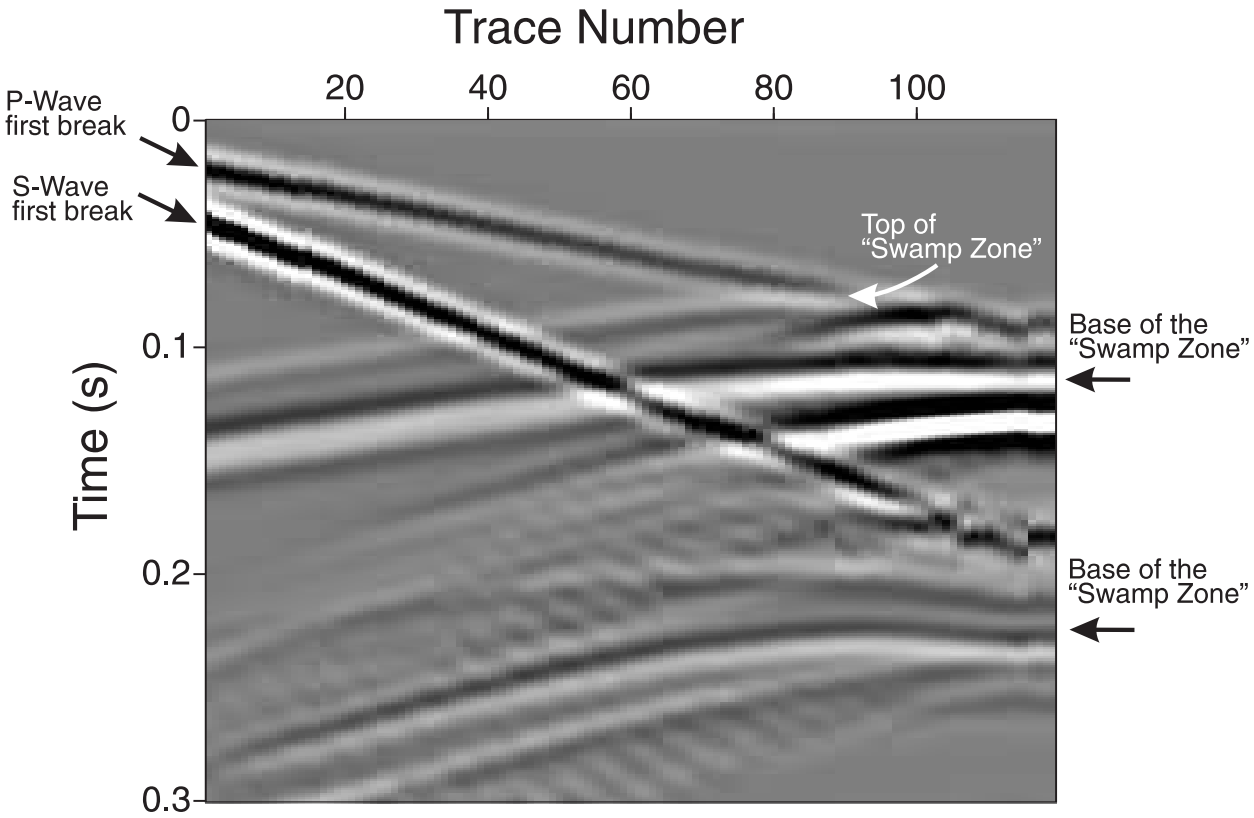

Figure 10: Modelling of the Cadieux VSP. This synthetic model includes P- and S-waves.

8.2 *In situ* measurements

Density and full waveform sonic data were collected to a depth of 558 m (Figure 13). The compressional wave (P-wave) was estimated by picking interactively the first arrivals on the near and far receivers. The P-wave velocity is calculated by dividing the distance that separates the two receivers by the delay between first arrival times. Velocity readings were obtained every 0.1 m. Velocities above 6 km/s were recorded in most of the rock units. Reduced P-wave velocities and densities were observed between 152 and 157 metres in a zone of fractured hematized dolomitic marble. Reduced P-wave velocities in the top 100 m are likely due to a combination of fracturing and alteration.

For the analysis of seismic reflectivity, acoustic impedance (the density - velocity product) becomes the most important parameter. Acoustic impedance contrasts control the strength of the seismic reflection response (*i.e.* contacts between lithological units of different acoustic impedances are likely to generate reflections). Impedances calculated from *in situ* densities and P-wave velocities are presented in Figure 13. Lower acoustic impedances are found in the top 100 m (fracturing and alteration), between 152 and 157 m (shear zone), and in a

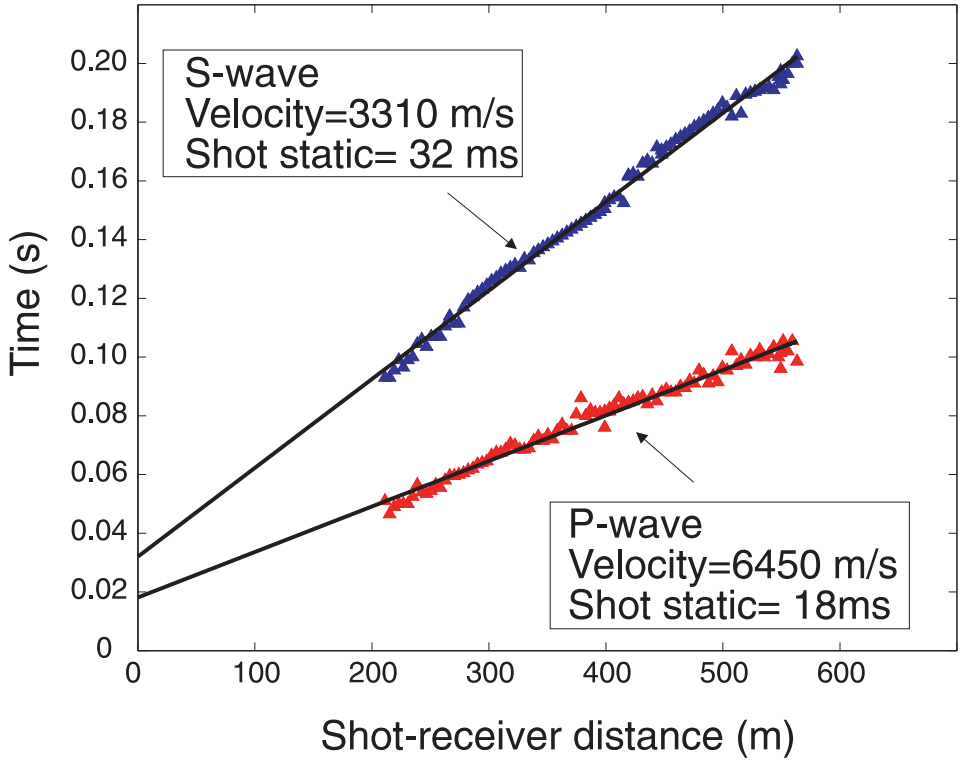

Figure 11: Result of the linear regression performed on the P-wave and S-wave VSP first break pick times. The intercept time is significantly different for the P- and S-wave, and suggests that the S-wave is generated at the source.

pegmatite unit located between 434 and 452 m.

In situ studies in borehole CA-96-01G confirm that lithological contacts are the source of seismic reflections. In particular, the pegmatite unit appears to be one of the strongest reflector. *In situ* physical rock properties of the Swamp Zone are inconclusive since only non-economical sulphides have been intersected by hole CA-96-01G.

8.3 Implications for exploration using seismic reflection methods

The DSI experiment at Cadieux demonstrates that the disseminated sulphides of the Swamp Zone cause the strongest seismic reflections. A 25 m thick pegmatite unit was also identified as a potential seismic reflector. The marbles and dolomitic marbles dominating the stratigraphy at Cadieux are quite homogeneous in terms of densities and seismic velocities and are likely to cause reflections only when they are in contact with pegmatites or disseminated sulphides. A deeper reflection was also clearly imaged on the P-wave section. Two possible origins are proposed for that reflection: an amphibolite unit intercepted at 660

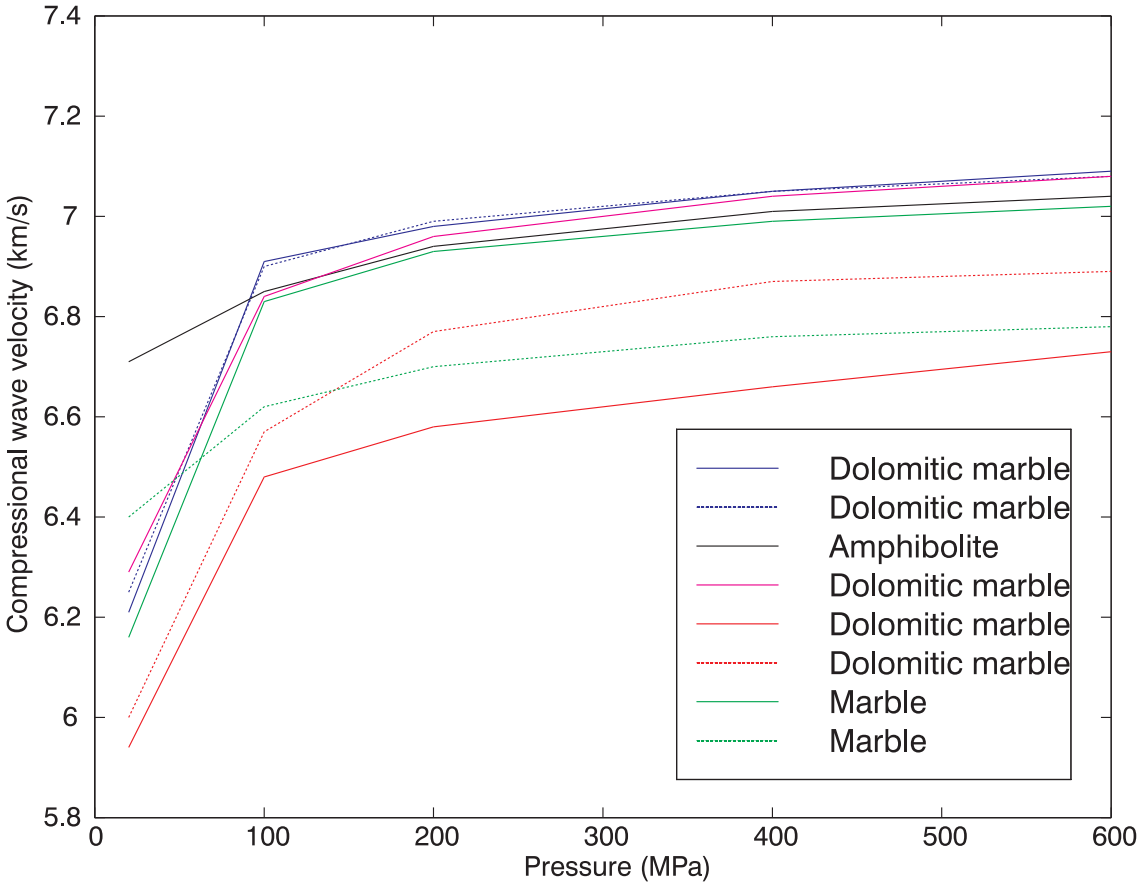

Figure 12: Diagram of the compressionnal wave velocity (P-wave) as a function of pressure.

m depth or the base of the mineralized zone seen as an offhole anomaly. Since no data have been acquired below 532 m, the ambiguity remains.

9 Conclusions

- Disseminated sulphides from the Swamp zone generate a strong reflection.
- Marbles and dolomitic marbles form a sequence of homogeneous rocks in terms of density and seismic velocity.
- Pegmatite and possibly amphibolite units can also generate strong reflections.
- An offhole amplitude anomaly has been identified at a depth of 300 m on the P-wave section. We believe that this anomaly is caused by local thickening of a pegmatite unit.

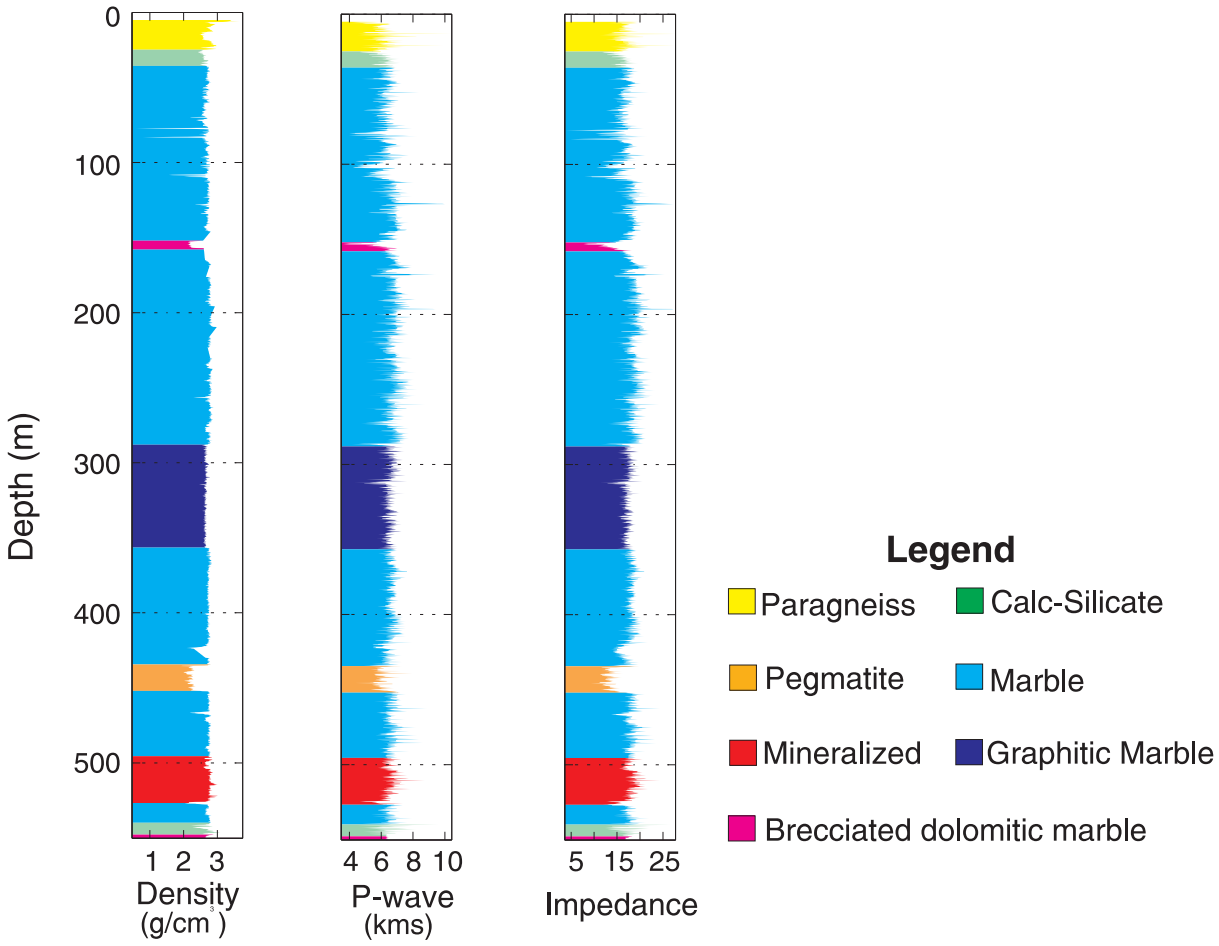

Figure 13: *In situ* density and P-wave velocity measurements in hole CA-96-01G. Seismic reflectivity is controlled by the acoustic impedance (the product of density and P-wave velocity). Clearly the pegmatites should generate the strongest reflections but there is no representative intersection of sulphides to estimate their reflectivity.

- With the water-filled shot point, 90 g pentolite boosters generate sufficient energy and high frequencies for this survey but for greater depths, a more powerful source would be preferable.

10 References

Adam, E. and Langlois P. 1995. Elimination of monofrequency noise from seismic records. Lithoprobe Seismic Processing Facility Newsletter, 8, pp.59-65.

Butler, K.E. and Russell, R.D. 1993. Subtraction of powerline harmonics from geophysical records. Geophysics, 58, pp.898-903.

Hardage, B. A., 1985. Vertical seismic profiling Part A: principles. Geophysical Press (London). 509 p.

Nyman, D.C. and Gaiser, J.E. 1983. Adaptive rejection of high-line contamination: 53 rd Ann. Internat. Mtg., Soc. Expl. Geophys., Expanded Abstracts, 321-323.

Roger, G. 1996. Report of field work - 1996, Cadieux Property Admaston township, Ontario. Unpublished Noranda Mining and Exploration internal report.